CIRCUM-PACIFIC MAP SERIES
MAP CP-38

DEPARTMENT OF THE INTERIOR
U.S. GEOLOGICAL SURVEY
Dallas L. Peck, Director

CIRCUM-PACIFIC COUNCIL FOR ENERGY AND MINERAL RESOURCES
Michel T. Halbouty, Chairman and President

CIRCUM-PACIFIC MAP PROJECT
John A. Reinemund, Director
George Gryc, General Chairman

GEODYNAMIC MAP OF THE CIRCUM-PACIFIC REGION

ARCTIC SHEET

GEORGE W. MOORE, CHAIRMAN, ARCTIC PANEL

FREE-AIR GRAVITY ANOMALIES
Richard H. Rapp, Department of Geodetic Science and Surveying, Ohio State University, Columbus, Ohio 43210, USA
EARTHQUAKE FOCAL MECHANISMS
Wilbur A. Rinehart, National Geophysical Data Center, National Oceanic and Atmospheric Administration, Boulder, Colorado 80303, USA
HOLOCENE VOLCANOES
Tom Simkin and Lee Siebert, National Museum of Natural History, Smithsonian Institution, Washington, D.C. 20560 USA

STATE OF LITHOSPHERIC STRESS
Mary Lou Zoback, U.S. Geological Survey, Menlo Park, California 94025, USA
HISTORICAL FAULTING
Manuel G. Bonilla, U.S. Geological Survey, Menlo Park, California 94025, USA
ACTIVE PLATE BOUNDARIES
George W. Moore, Department of Geosciences, Oregon State University, Corvallis, Oregon 97331, USA
CRUSTAL THICKNESS
David R. Soller, U.S. Geological Survey, Reston, Virginia 22092

MAP PRODUCTION BY THE U.S. GEOLOGICAL SURVEY
Compilation Coordinated by George Gryc
Cartography by Frank J. Sidlauskas, Jr.

SCALE 1:10 000 000

(Map center point 70° N., 165° W.)
Lambert Azimuthal Equal Area Projection

1990

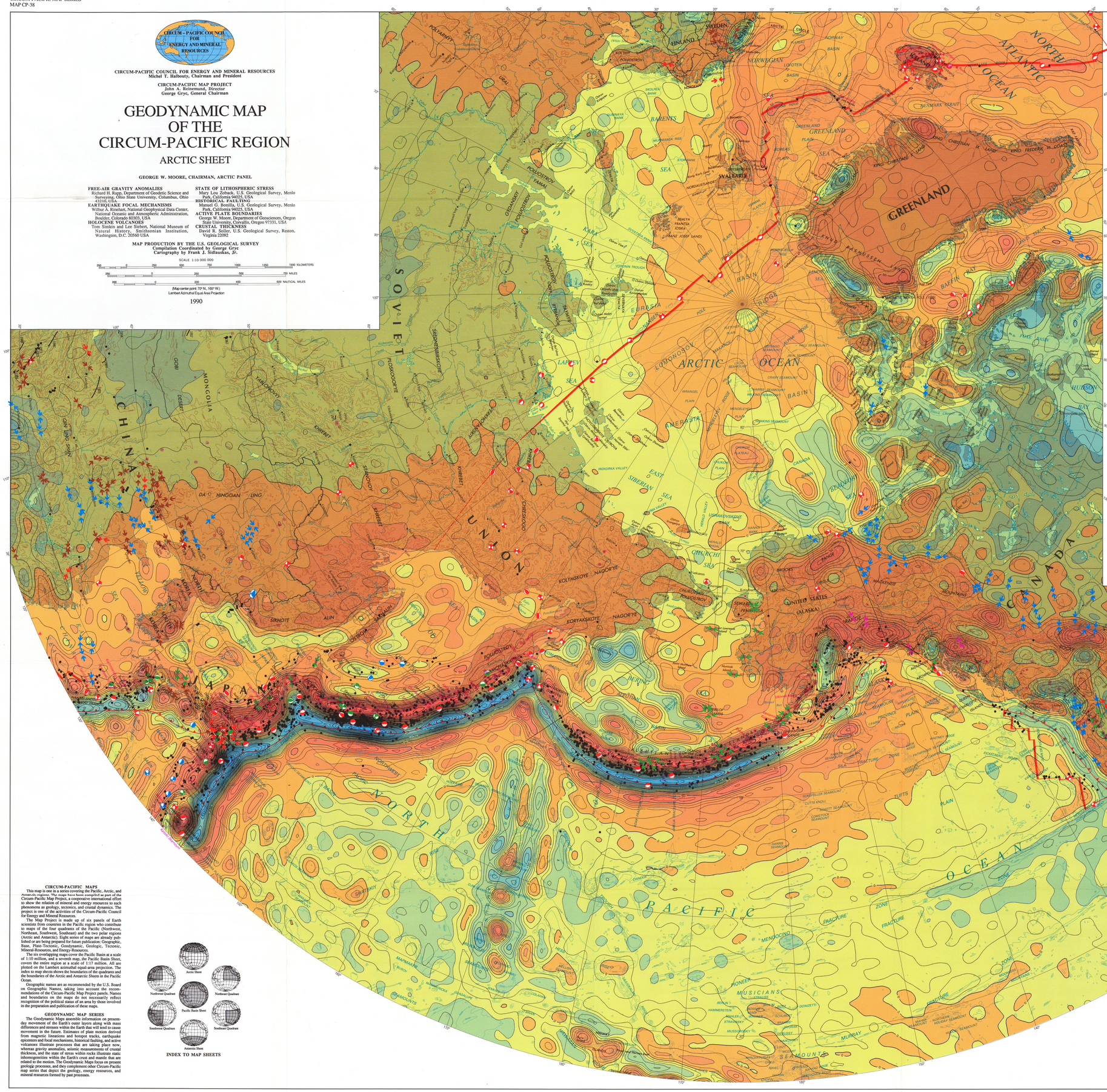

EXPLANATION

GRAVITY ANOMALIES

Free-air anomalies (10⁻⁵ ms⁻²): 200, 100, 50, 20, 0, -20, -50, -100, -200

STATE OF LITHOSPHERIC STRESS (Maximum horizontal compressive stress direction)

- **Hydraulic fracturing**—Measured parallel to a vertical tensile fracture that formed when a borehole was artificially pressurized.
- **Wellbore breakouts**—Measured perpendicular to the mean azimuth of stress-induced spalling of the wall of a borehole.
- **Borehole overcoring**—Measured parallel to the maximum strain-release direction after overcoring.
- **Quaternary slickensides**—Determined from the sense and orientation of slip vectors measured on two or more surfaces within an active fault zone.
- **Volcano alignment**—Measured parallel to the trend of five or more contemporaneous aligned Quaternary volcanic centers.

EARTHQUAKE FOCAL MECHANISMS

Depth (km): 0, 70, 300, 700

Focal depth—Marked by the color of the symbol, which is a stereographic projection of nodal planes intersecting the lower hemisphere of the focal sphere, on which compressional first-motion quadrants are colored.

Type of faulting—Maximum horizontal compression direction indicated by arrows; strike-slip faulting can be expressed as shear, in the example either right-lateral if the fault extends from top to bottom, or left-lateral if from left to right; in normal faulting, the vertical compression axis is shortest and the horizontal, and the rock mass to spread horizontally, in the example from left to right.

Normal faulting; Normal faulting with a strike-slip component; Strike-slip faulting; Thrust faulting with a strike-slip component; Thrust faulting

EARTHQUAKES

Epicenters—Magnitude 5.7 and greater events during 1964 through 1987

HISTORICAL FAULTING

1875 — **Faults**—Labels indicate date of rupture.

ACTIVE TECTONIC PLATES

Transform fault; Subduction Zone; Spreading axis — **Plate boundaries**—Interrupted where coincident with historical faulting; teeth on upper plate at subduction zones.

VOLCANIC CENTERS

- **Active in historic time**—Generally within past 1,000 yr, and documented during or soon after eruption; volcano named in color if active 1964 through 1988.
- **Active in Holocene time**—Within past 10,000 yr; not documented historically.
- **Holocene activity uncertain**—Includes solfataras and volcano-related thermal springs; no direct evidence for Holocene eruption.

BASE MAP

- **Topographic contours**—Altitude in meters.
- **Bathymetric contours**—Depth of water in meters.
- City—1,000,000 or more people
- City—less than 1,000,000 people

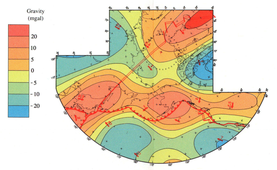

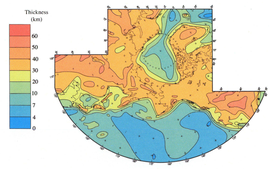

FREE-AIR GRAVITY (TO DEGREE 10)

This map is based on a spherical harmonic expansion to degree 10 of the data set that was used for the main map to degree 180 (Rapp and Cruz, 1986). Whereas the gravity contours on the main map are especially sensitive to subsurface density differences that create surface gravity anomalies with wavelengths of the order of 1° of latitude and longitude (approximately 100 km), the higher harmonics have been neglected on this inset map, making its contours most sensitive to wavelengths of about 20° (2,000 km). The depth to which density differences below the surface can be sensed is of the order of the wavelengths of the anomalies, so the main map reveals density contrasts mainly in the crust (30 km) and its enclosing lithospheric plate (100 km), whereas this map reveals them in the zone from near the roots of subduction zones (4500 km) to the core-mantle interface (2,900 km). This map also shows the rates and directions of movement of the active lithospheric plates with respect to the lower mantle, as inferred by Minster and Jordan (1978) from traces of active hotspots and from 330 relative-motion determinations of rate from seafloor spreading and direction from transform faults and earthquake first-motion analyses.

SOURCES OF DATA

GRAVITY ANOMALIES
The free-air anomalies were derived from a set of potential coefficients that were estimated by combining coefficients implied by the perturbations of satellite orbits with mean free-air terrestrial anomalies for 30x30-minute areas of latitude and longitude and with mean anomalies for matching ocean areas derived from satellite radar altimeter data (Rapp and Cruz, 1986). This information yielded an set of potential coefficients which were used to degree and order 180. The anomalies were computed on a 0.5x0.3° grid from which the contours were plotted.

FOCAL MECHANISMS
The source of the data is the focal-mechanism file of the National Earthquake Information Center, U.S. Geological Survey, supplemented by data in Jemsek et al (1986) and Fujita et al (in press), and by unpublished data from S. I. Sherman, Institute of the Earth's Crust, Irkutsk, and Z. Xu, Institute of Geophysics, Beijing. The positions were plotted by computer at the National Geophysical Data Center, National Oceanic and Atmospheric Administration. The symbols, drawn on a laser printer, are oriented with respect to local north, regardless of map projection.

HOLOCENE VOLCANOES
Plotted with additions from the computerized Smithsonian Institution Volcano Reference File (Simkin et al, 1981) by the U.S. Geological Survey, Reston, Virginia. The contributions to the file by Lindsay McClelland, Smithsonian Institution, and John H. Latter, New Zealand Department of Scientific and Industrial Research and by many compilers of the International Association of Volcanology and the Volcanological Society of Japan are especially acknowledged. Submarine-rift volcanism is not included.

LITHOSPHERIC STRESS
Compiled and plotted from the U.S. Geological Survey lithospheric-stress data file using the guidelines and criteria for stress indicators outlined by Zoback and Zoback (1980). Earthquake focal mechanisms have been used where they are the only stress indicators in another map element. The directions of the opposed arrows represent the true azimuths of the maximum horizontal compressive stress direction, taking account of the distortion in the map projection.

HISTORICAL FAULTING
The principal sources for the onshore faults that are reported to have been active during historic time, and which are printed in black, are Bell (1984), Bonilla et al (1980), Clark et al (1982), Crone et al (1987), Deng and Wang (1984), Emerson et al (1981), Geological Survey of Japan (1982, 1983 et al (1980), Howard et al (1978), Lienkaemper et al (1987), Nakata and Deng (1984), Nikolaev (1984), and Sharp et al (1980), and segments of active plate boundaries that are not accompanied by known historic displacement are printed in red and are not separately distinguished from other onshore and offshore segments of plate boundaries where historic displacement is not a matter of record. Long-term creep is not included, but displacement from subsurface rupture that propagated to the surface soon after a major earthquake is included.

ACTIVE PLATE BOUNDARIES
Adapted from the revised third edition of the Northeast Quadrant (1986) and the Northwest Quadrant (1987) of the Plate-Tectonic Map of the Circum-Pacific Region, and from Vogt (1986), taking account of the earthquakes and bathymetry on this map.

EARTHQUAKE EPICENTERS
Adapted from the Arctic Sheet of the Plate-Tectonic Map of the Circum-Pacific Region (1987), in which the earthquakes are distinguished by focal depth (W. A. Rinehart, in preparation).

CRUSTAL THICKNESS
Updated from a data set compiled from seismically-derived crustal thickness values (Soller et al, 1982), and incorporating data from Priev and Yanshin (1980). Because of the irregular and commonly sparse data distribution, the positions of continental margins (as indicated on bathymetric maps) and plate boundaries were used in places as an aid in contouring.

BASE MAP
From the Arctic Sheet of the Geographic Map of the Circum-Pacific Region (1990), on which the bathymetry was compiled by Frank J. Sidlauskas, Jr., U.S. Geological Survey, Reston, Virginia, and the topography by Thomas A. Brikham, Department of Geosciences, Oregon State University, Corvallis, Oregon. Latitude and longitude grid lines, shorelines, and drainage are computer plotted.

CRUSTAL THICKNESS

The depth to the Mohorovičić discontinuity (moho), which marks the boundary between the Earth's crust and mantle, was determined mainly on the basis of abrupt changes in seismic velocity at that depth (Soller et al, 1982). The velocity at the moho changes downward from about 6.9 to 8.1 km/s, and this change is equated on the basis of laboratory experiments to a change in rock density from about 2.8 to 3.4 g/cm³. Oceanic crust averages about 6 km thick, and continental crust about 35 km, although the crust along mountain ranges is thicker. The thickest crust in the world, at the Himalaya, exceeds 80 km, probably because two or more layers of continental crust became stacked together when India collided with Asia. Presumed outcrops of the oceanic moho at sites of former continental collision suggest that the rock directly above the oceanic moho is gabbro and that below is peridotite, rock types whose densities match those inferred from the seismic velocities measured at depth. Regional variations in thickness revealed by this new compilation, both in the ocean basins and on the continents provide additional information for interpreting the geodynamic significance of the other elements in this map series.

REFERENCES CITED

Bell, J. W., 1984, Quaternary fault map of Nevada—Reno Sheet: Nevada Bureau of Mines and Geology, Map 79.
Bonilla, M. G., J. J. Lienkaemper, and J. C. Tinsley, 1980, Surface faulting near Livermore, California, associated with the January 1980 earthquakes: U.S. Geological Survey Open-File Report 80-723, 32 p.
Clark, M. M., J. C. Yount, P. R. Vaughan, and R. L. Zepeda, 1982, Map showing surface ruptures associated with the Mammoth Lakes, California, earthquakes of May 1980: U.S. Geological Survey Miscellaneous Field Studies Map MF-1396, scale 1:24,000.
Crone, A. J., M. N. Machette, M. G. Bonilla, J. J. Lienkaemper, K. L. Pierce, W. E. Scott, and R. C. Bucknam, 1987, Surface faulting accompanying the Borah Peak earthquake and segmentation of the Lost River fault, central Idaho: Seismological Society of America Bulletin, v. 77, p. 739-770.
Deng, Q., and Y. Wang, 1984, Principal features of neotectonics in China, in K. Hirzio, ed., Tectonic belts of Asia: Tokyo, Kaihun-do, p. 29-89.
Eissler, H. K., L. Jones, E. Hauge, J. Dewey, R. Stefansson, and T. Skafladitir, 1981, Seismicity pattern in the south Iceland seismic zone, in Simpson, D. W., and Richards, P. G., eds., Earthquake prediction—an international review: American Geophysical Union Maurice Ewing Series, v. 4, p. 141-151.
Fujita, K., D. B. Cook, H. Hasegawa, D. Forsyth, and R. Wennillie, in press, Seismicity and focal mechanisms of the Arctic region and the North American plate boundary in Asia: Geological Society of America Geology of North America, v. L.
Geological Survey of Japan, 1982, Active fault distribution map: Geological Atlas of Japan, p. 58-59.
Hill, R. L., J. A. Treiman, J. W. Given, J. C. Fechmann, J. R. McMillan, and J. E. Ebel, 1980, Geologic Study of the Homestead Valley earthquake swarm of March 15, 1979: California Geology, v. 33, p. 60-67.
Howard, K. A., et al, 1978, Preliminary map of young faults in the United States as a guide to earthquakes—Sheet 2, Western United States: U.S. Geological Survey Map MF-916, scale 1:5,000,000.
Jemsek, J. P., E. A. Bergman, I. L. Nabelek, and S. C. Solomon, 1986, Focal depths and mechanisms of large earthquakes on the Arctic mid-ocean ridge system: Journal of Geophysical Research, v. 91, p. 13,993-14,005.
Lienkaemper, J. J., S. K. Pezzopane, M. M. Clark, and M. J. Rymer, 1987, Fault fractures formed in association with the 1986 Chalfant Valley, California, earthquake sequence: preliminary report: Seismological Society of America Bulletin, v. 77, p. 297-305.
Minster, J. B., and T. H. Jordan, 1978, Present-day plate motions: Journal of Geophysical Research, v. 83, p. 5331-5354.
Molnar, P., and Q. Deng, 1984, Faulting associated with large earthquakes and the average rate of deformation in central and eastern Asia: Journal of Geophysical Research, v. 89, p. 6203-6227.
Moritz, H., 1980, Geodetic Reference System 1980: Bulletin Geodesique, v. 54, p. 395-405.
Priev, A. V., and A. L. Yanshin, 1980, Scheme of distribution of continental crusts of various ages in northern Eurasia and relief of the 'moho' surface, in Tectonic Map of Northern Eurasia: USSR Academy of Sciences, scale 1:1,500,000.
Rapp, R. H., and J. Y. Cruz, 1986, Spherical harmonic expansions of the Earth's gravitational potential to degree 360 using 30' mean anomalies: Ohio State University Department of Geodetic Science and Surveying Report 376, 25 p.
Rymer, M. J., K. K. Harms, M. M. Clark, and J. J. Lienkaemper, 1984, Surface faulting associated with the June 11 aftershock of the May 2, 1983, Coalinga earthquake [California]: Earthquake Engineering Research Institute Report 84-03, p. 57-60.
Sharp, R. V., K. E. Budding, J. Boatwright, M. J. Ader, M. G. Bonilla, M. M. Clark, T. E. Fumal, K. K. Harms, J. J. Lienkaemper, D. M. Morton, B. J. O'Neill, C. L. Ostergren, D. J. Ponti, M. J. Rymer, J. L. Saxton, and J. D. Sims, 1989, Surface faulting along the Superstition Hills fault zone and nearby faults associated with the earthquakes of 24 November 1987: Seismological Society of America Bulletin, v. 79, p. 252-281.
Simkin, T., L. Siebert, L. McClelland, D. Bridge, C. Newhall, and J. H. Latter, 1981, Volcanoes of the world—a regional directory, gazetteer, and chronology of volcanism during the last 10,000 years: Stroudsburg, Penna., Hutchinson Ross, 232 p.
Soller, D. R., R. D. Ray, and R. D. Brown, 1982, A new global crustal thickness map: Tectonics, v. 1, p. 125-149.
Vogt, P. R., 1986, Portrait of a plate boundary: the Mid-Atlantic Ridge from the Equator to Siberia: Geological Society of America Geology of North America, v. M, plate 8A, scale 1:13,888,000.
Zoback, M. L., and M. D. Zoback, 1980, State of stress in the conterminous United States: Journal of Geophysical Research, v. 85, p. 6113-6156.

CIRCUM-PACIFIC MAPS

This map is one in a series covering the Pacific, Arctic, and Antarctic regions. The maps have been compiled as part of the Circum-Pacific Map Project, a cooperative international effort to show the relation of mineral and energy resources to such phenomena as geology, tectonics, and crustal dynamics. The project is one of the activities of the Circum-Pacific Council for Energy and Mineral Resources.

The Map Project is made up of six panels of Earth scientists from countries in the Pacific region who contribute to maps of the four quadrants of the Pacific (Northwest, Northeast, Southwest, Southeast) and the two polar regions (Arctic and Antarctic). Eight series of maps are already published or are being prepared for future publication: Geographic, Base, Plate-Tectonic, Geodynamic, Geologic, Tectonic, Mineral-Resources, and Energy-Resources.

The six overlapping maps cover the Pacific Basin at a scale of 1:10 million, and a seventh map, the Pacific Basin Sheet, covers the entire region at a scale of 1:17 million. All are plotted on the Lambert azimuthal equal-area projection. The index to map sheets shows the boundaries of the quadrants and the boundaries of the Arctic and Antarctic Sheets in the Pacific Ocean.

Geographic names are as recommended by the U.S. Board on Geographic Names, taking into account the recommendations of the Circum-Pacific Map Project panels. Names and boundaries on the maps do not necessarily reflect recognition of the political status of an area by those involved in the preparation and publication of these maps.

GEODYNAMIC MAP SERIES

The Geodynamic Maps assemble information on present-day movement of the Earth's outer layers along with mass differences and stresses within the Earth that will tend to cause movement in the future. Estimates of plate motion derived from magnetic lineations and hotspot tracks, earthquake epicenters and focal mechanisms, historical faulting, and active volcanoes illustrate processes that are taking place now, whereas gravity anomalies, seismic measurements of crustal thickness, and the state of stress within rocks illustrate static inhomogeneities within the Earth's crust and mantle that are related to the motion. The Geodynamic Maps focus on present geologic processes, and they complement other Circum-Pacific map series that depict the geology, energy resources, and mineral resources formed by past processes.

INDEX TO MAP SHEETS

Base by U.S. Geological Survey, 1989

INTERIOR—GEOLOGICAL SURVEY, RESTON VIRGINIA—1990

For sale by Branch of Distribution, U.S. Geological Survey, Box 25286, Federal Center, Denver, CO 80225